Surface and subsurface oxygen vacancies in anatase TiO_2 and differences with rutile

Hongzhi Cheng and Annabella Selloni
Department of Chemistry, Princeton University, Princeton, New Jersey 08540, USA
(Received 8 December 2008; published 16 March 2009)

First-principles density-functional theory calculations in the generalized gradient approximation are carried out to study the relative stabilities of oxygen vacancies at surface and subsurface sites of anatase TiO_2(101) and TiO_2(001), and, for comparison, of the prototypical rutile TiO_2(110) surface. Our results indicate that these defects are significantly more stable at subsurface than at surface sites in the case of anatase surfaces, whereas bridging oxygen sites are favored for O vacancies at rutile TiO_2(110). Also, calculations of O-vacancy diffusion pathways at anatase TiO_2(101) show that the energy barrier to diffuse from surface-to-subsurface sites is sufficiently low to ensure a rapid equilibration of the vacancy distribution at typical surface annealing temperatures. These results could explain why, experimentally, anatase surfaces are found to have a significantly lower defect concentration and/or to be more difficult to reduce than those of rutile.

DOI: 10.1103/PhysRevB.79.092101 PACS number(s): 68.35.Dv, 68.47.Gh, 71.15.Nc

Titanium dioxide (TiO_2) is a technologically important material, which is widely applied in photocatalysis[1] and solar energy conversion.[2] Since surfaces have a key role in all these applications, there has been an increasing interest in the fundamental physical and chemical properties of TiO_2 surfaces over the last decade.[3] The two most common TiO_2 polymorphs are rutile (**R**-TiO_2) and anatase (**A**-TiO_2). While **R**-TiO_2 is the thermodynamically most stable bulk phase, most nanomaterials are of **A**-TiO_2 form; moreover, below a particle size of ~14 nm,[4,5] the **A**-TiO_2 phase appears to be stabilized compared to **R**-TiO_2, an effect that is attributed to the lower surface energy of **A**-TiO_2 with respect to **R**-TiO_2.[4–6] Moreover, **A**-TiO_2 is typically found to be more effective in photocatalytic and photovoltaic applications, a fact for which no clear and widely accepted explanation is available yet.

Experimental investigations on well defined **A**-TiO_2 surfaces are still relatively sparse mainly because single **A**-TiO_2 crystals of sufficiently large size are difficult to grow. However, available studies of **A**-TiO_2(101) and **A**-TiO_2(001)—the majority and minority surfaces, respectively, in the **A**-TiO_2 Wulff shape[6]—have found that these surfaces have a significantly lower defect concentration and/or are more difficult to reduce than the prototypical **R**-TiO_2(110) surface under similar preparation conditions (see, e.g., Refs. 3 and 7 and references therein). Defects, in particular oxygen vacancies, have been known for long time to have a central role in the surface chemistry of oxide materials. On **R**-TiO_2(110), the concentration of O vacancies (V_O's) is quite large (5%–10%) under standard preparation conditions, and their structural and electronic properties have been the subject of intense investigation and debate in recent years.[3,8–13] V_O's are also important in the sputtering and annealing processes that are generally used for surface preparation: the diffusion of these defects, and of Ti interstitials (Ti_i's), largely determines the mass transport occurring between the surface and the bulk,[14] as well as the surface restructuring that often results from these processes (see, e.g., Ref. 15 and references therein).

The low defect density that is observed on **A**-TiO_2 surfaces, while in line with the high surface stability inferred from calorimetric measurements,[4] is not straightforward to understand. TiO_2 samples used in experiments are generally reduced, and should thus contain a substantial amount of V_O and Ti_i defects. Ti interstitials prefer to have a high coordination and therefore are mostly found in the bulk. For V_O's, instead, undercoordinated surface sites, where a smaller number of Ti-O bonds needs to be broken, should be energetically favored. Thus these defects should be frequent on the **A**-TiO_2 surface, as found indeed on **R**-TiO_2(110).

To rationalize the different V_O concentrations observed on the **R**-TiO_2(110) and **A**-TiO_2(101) surfaces, it was suggested that the surface V_O formation energy may be larger for the latter.[3] In fact, the removal of a surface twofold bridging oxygen (O_{2c}) results in two fivefold coordinated Ti (Ti_{5c}) cations on **R**-TiO_2(110) vs one Ti_{5c} and one fourfold Ti (Ti_{4c}) on the **A**-TiO_2(101) surface. Although numerous first-principles investigations of O vacancies on TiO_2 surfaces have been reported (see, e.g., Refs. 10, 11, and 16–21), the differences between V_O defects at **R**-TiO_2 and **A**-TiO_2 surfaces have not yet been addressed by any theoretical study. These differences are the primary focus of the present study.

As a first step toward a better understanding of the behavior of O vacancies in **A**-TiO_2, we have performed extensive density-functional theory (DFT) calculations at the generalized gradient approximation (GGA) level to determine the energetics of these defects at different surface and subsurface sites, focusing on the majority **A**-TiO_2(101) surface but considering also **A**-TiO_2(001) and, as a reference, the **R**-TiO_2(110) surface. The limitations of DFT-GGA in describing the electronic structure of V_O defects in TiO_2 have been discussed in several recent publications (see, e.g., Refs. 10, 11, and 22–24) and largely originate from the self-interaction error of the approximate DFT functionals.[25] Some of these difficulties can be mitigated by the use of hybrid functionals or DFT+U methods.[10,22–24] While it would be valuable to carry out calculations of surface and subsurface defects using such approaches, the present study based on the use of a semilocal functional is both interesting on its own and also a first essential step for any further investigation.

In agreement with recent first-principles studies[17,19] and consistent with the simple argument given above, in this work we find that for **R**-TiO_2(110) the formation energy of surface O_{2c} vacancies is lower than that of subsurface V_O's. For both **A**-TiO_2(001) and **A**-TiO_2(101) surfaces, instead,

we find that O vacancies have lower formation energy in the subsurface than at the surface. In addition, we determined the V_O's surface-to-subsurface diffusion pathways for **A**-TiO_2(101) and found that the corresponding barriers are rather low. This suggests that surface V_O defects, once formed, can easily diffuse to the subsurface, consistent with the low density of defects that is experimentally observed on the **A**-TiO_2 surface.

We carried out our DFT-GGA calculations using the Perdew-Burke-Ernzerhof (Ref. 26) exchange-correlation functional. As in previous studies based on semilocal functionals (see, e.g., Refs. 16 and 18), the effect of spin polarization was found irrelevant in a few test cases, and therefore was not included in subsequent calculations. We used the plane-wave-pseudopotential scheme[27] with ultrasoft pseudopotentials[28] and a kinetic-energy cutoff of 25 (200) Ry for the smooth part of the wave functions (augmented density). All surfaces were modeled using repeated slab geometries with a vacuum of ~11.5 Å width between slabs. For each surface we considered at least two different slab models in order to check the dependence on cell size, e.g., we used slabs of three and six TiO_2 layers containing 108 and 216 atoms, respectively, for **A**-TiO_2(101), slabs of four and six TiO_2 layers containing 96 and 144 atoms, respectively, for **R**-TiO_2(110), and two different slabs of four TiO_2 layers containing 102 and 153 atoms for the **A**-TiO_2(001) surface. For the latter we took the widely accepted (1×4) admolecule (ADM) reconstruction model of Ref. 29. Due to the large sizes of these systems, only Γ was used to sample k space; test calculations on a 72-atom **A**-TiO_2(101) slab showed negligible (~0.03 eV) differences between the formation energies of surface and subsurface defects determined with a $2\times2\times1$ k-point mesh and those obtained using only Γ. In the structural optimizations, residual forces were $\leq$0.05 eV/Å. O-vacancy formation energies (E_{form}) were determined from the expression: $E_{form}(V_O)=E_{tot}(def)-E_{tot}(no\ def)+\frac{1}{2}\mu(O_2)$, where $\mu(O_2)$ is the total energy of an O_2 molecule, and E_{tot} (def) and E_{tot} (no def) are the total energies of the system with and without defects, respectively. For simplicity and as in most theoretical studies of O vacancies in TiO_2, in this work we do not consider the dependence on the oxygen chemical potential. The procedure of comparing formation energies at different sites of the same supercell allows us to minimize the influence of technical details so that the comparison is much more meaningful than for calculations performed with different setups.

The computed formation energies for several inequivalent surface and subsurface V_O defects at the **A**-TiO_2(101) surface are reported in Table I (see Fig. 1 for the labeling of the sites). On the surface, V_{O1}, corresponding to the removal of an O_{2c}, is the energetically most favorable V_O defect. Among subsurface sites, the site directly below the surface O_{2c} (not reported in Table I) is found to be unstable: if a vacancy is created at that site, the O_{2c} atom just above it moves spontaneously to fill the vacancy, leaving a surface V_{O1} defect. The most interesting feature of the results in Table I, however, is that the formation energy of the subsurface V_{O4} defect is lower than that of V_{O1} at the surface. To test the reliability of this result initially obtained with the smaller slab of 108 atoms, the calculations were repeated using the thicker **A**-TiO_2(101) slab containing 216 atoms [Fig. 1(a)]. The resulting formation energies for the surface (V_{O1}), first subsurface (V_{O4}), and second subsurface (V_{O5}) sites are 4.15, 3.69, and 3.65 eV, respectively. The energies for the two subsurface sites are almost identical to one to the other, suggesting that these sites may be already considered "bulklike." The difference in stability, $\Delta E\sim0.5$ eV, between surface and subsurface sites corresponds to a relative probability of V_O being at the surface of $\sim4\times10^{-9}$ and 1.6×10^{-3} at $T=300$ and 900 K, respectively.

By comparing the results obtained with the thinner (108 atoms) and thicker (216 atoms) slabs in Table I, we can see that, while for V_{O1} the formation energy does not depend significantly on slab size, for V_{O4} E_{form} is 0.34 eV smaller for

TABLE I. Formation energies, in eV, of V_O defects at different surface and subsurface sites of **A**-TiO_2(101), **A**-TiO_2(001), and **R**-TiO_2(001), as defined in Fig. 1, and calculated using slab models containing 216 (108), 153 (102), and 144 (96) atoms, respectively. For each surface, the defects with lowest formation energies are in bold.

Defect site	**A**-TiO_2(101)	**A**-TiO_2(001) (1×4)	**R**-TiO_2(110)
V_{O1}	4.15(4.25)	4.57(4.72)	**3.68**(4.01)
V_{O2}	(5.40)	5.17(5.52)	4.50(4.56)
V_{O3}	(4.73)	4.29(5.05)	**3.99**(4.23)
V_{O4}	**3.69**(4.03)	4.78(5.08)	5.23(5.22)
V_{O5}	**3.65**	**4.10**(4.34)	4.73(4.83)
V_{O6}			5.28(5.29)
V_{O7}			4.46
V_{O8}			4.67
V_{O9}			4.38

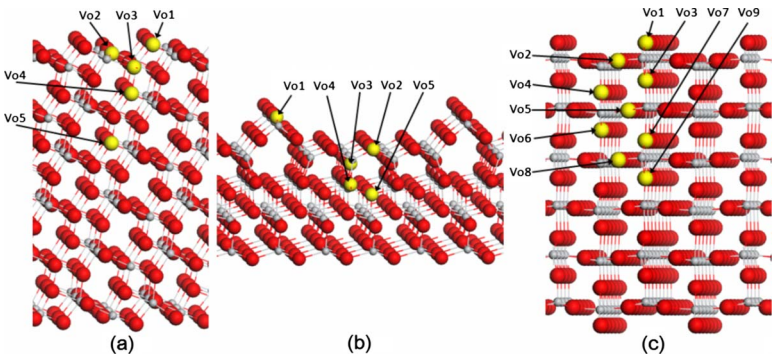

FIG. 1. (Color online) Slab models and O-vacancy sites (highlighted in yellow) considered in this work. (a) **A**-TiO_2(101) surface, slab model with six TiO_2 layers. (b) (1×4)-reconstructed **A**-TiO_2(001) surface, slab model with four TiO_2 layers. (c) **R**-TiO_2(110) surface, slab model with six TiO_2 layers. Oxygen are red and Ti atoms are gray.

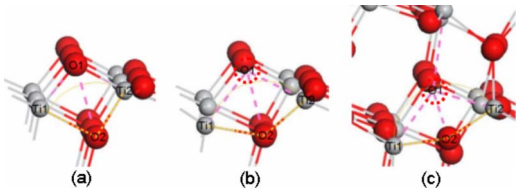

FIG. 2. (Color online) Optimized atomic structures: (a) before and (b) after creation of a surface O vacancy [V_{O1} in Fig. 1(a)]; (c) after creation of a subsurface O vacancy [V_{O4} in Fig. 1(a)] at the **A**-TiO_2(101) surface. A few relevant atoms are indicated. O1, the atom that is removed to create the vacancy, is indicated by a dashed red circle in (b) and (c). Bond distances and angles are reported in Table II.

the thicker slab because this allows for a better local relaxation around the vacancy site. This result also provides the key for understanding why O vacancies prefer to stay in subsurface rather than at the surface of anatase. Indeed, analysis of the structural relaxations around the vacancy sites shows much larger atomic displacements in the subsurface region than at the surface (see Fig. 2 and Table II). The surface is very "rigid," as indicated also by the short bond lengths formed by O_{2c} with the neighboring Ti atoms. These short bond lengths enhance the stability of the surface but at the same time also lead to a very high energy cost for creating a defect.

For completeness, we also determined the V_O diffusion pathways between the different surface and subsurface sites on **A**-TiO_2(101). To this end, nudged-elastic-band (NEB) (Ref. 30) calculations were performed using a slab of three TiO_2 layers containing 72 atoms, and k space was sampled with a $2\times2\times1$ k-point mesh. For each set of initial and final states, different pathways were explored in order to determine the most favorable one. The barriers along the most favorable pathways are reported in Table III. V_O diffusion on the surface appears to be largely inhibited; in particular, the direct surface $V_{O1}\rightarrow V_{O1}$ diffusion barrier along [010] is substantial, ~2.65 eV. This is quite different from **R**-TiO_2(110), where scanning tunneling microscopy (STM) measurements and DFT calculations found that O_{2c} vacancies have a surface diffusion barrier of only ~1.1 eV.[12] Instead, a much lower barrier (0.74 eV) is found for diffusion from the surface to the subsurface, $V_{O1}\rightarrow V_{O4}$. This indicates that this pathway can be easily accessed under annealing conditions, thus allowing for rapid equilibration of the defect density between surface and subsurface sites. Selected atomic configurations along the pathway are shown in Fig. 3. We can see a two-atom diffusion mechanism, in which the sub-bridging oxygen (i.e., the O atom directly below O_{2c}) moves up to fill the V_{O1} vacancy while the site that it leaves vacant is filled by the O atom initially in the V_{O4} site. Note that Table III reports a barrier of 0.95 eV for the reverse $V_{O4}\rightarrow V_{O1}$ process. Taking into account that the slab model used for the barrier calculations underestimates the relative stability of V_{O1} and V_{O4} by ~0.3 eV, a more realistic estimate for this reverse diffusion barrier is ~1.25 eV. This is substantially larger than the barrier for the direct process, confirming that defects tend to remain confined in the subsurface region.

Turning now to a more detailed comparison with experiment, our first-principles results for the O-vacancy formation energies on **A**-TiO_2(101) agree with the low concentration of O vacancies experimentally observed by STM and temperature programed desorption (TPD) on this surface.[3] Recent ultraviolet photoemission spectroscopy (UPS) measurements, showing a high concentration of V_O induced gap states following bombardment and annealing of **A**-TiO_2(101),[7] can be also understood on the basis of our results: the observed defect states may be indeed assigned to vacancies in the subsurface region which is accessed by UPS measurements and where the V_O's prefer to reside according to our calculations. In the same UPS study,[7] however, comparison of the electronic structures of **A**-TiO_2(101), **A**-TiO_2(001), and **R**-TiO_2(110) as a function of V_O defect concentration shows that, under similar preparation conditions, **A**-TiO_2(101) has the highest concentration of defects, somewhat higher than **R**-TiO_2(110), whereas **A**-TiO_2(001) exhibits an extremely low concentration of V_O's. To obtain insights into these findings, the energetic of surface and subsurface V_O's on the (1×4)-reconstructed[29] **A**-TiO_2(001) surface and, for comparison, on **R**-TiO_2(110) was studied with the same methodology and computational setup used for **A**-TiO_2(101). The results are also reported in Table I (site labeling shown in Fig. 1).

By comparing first the results for the two **A**-TiO_2 surfaces, we can see that, similarly to what was found on

TABLE II. Bond distances (in Å) and bond angles (in degrees) before (I, III, V) and after (II, IV, VI) creation of an O vacancy at the **A**-TiO_2(101) surface. (I, II) Surface V_{O1}; (III, IV) subsurface V_{O4}; (V, VI) second subsurface V_{O5} [see Fig. 1(a) for definition of V_O sites]. Atoms are labeled as in Fig. 2.

	O1-Ti1	O1-Ti2	O2-Ti1	O2-Ti2	Ti1-O2-Ti2
I	1.845	1.831	2.069	1.784	94.22
II	2.250	2.138	1.951	1.802	129.03
III	1.918	1.938	1.991	1.865	98.94
IV	2.245	2.094	1.833	1.802	154.56
V	1.929	1.951	1.988	1.901	99.96
VI	2.198	2.129	1.811	1.803	167.74

TABLE III. Diffusion barriers (E^A) along the most favorable pathways connecting V_O binding sites at or near the **A**-TiO_2(101) surface. Calculations performed using a slab of 72 atoms.

	E^A (eV)	
	direct path	inverse path
$V_{O1}\rightarrow V_{O1}$	2.65	2.65
$V_{O1}\rightarrow V_{O2}$	1.34	0.30
$V_{O1}\rightarrow V_{O3}$	1.34	0.78
$V_{O2}\rightarrow V_{O3}$	0.30	0.78
$V_{O1}\rightarrow V_{O4}$	0.74	0.95
$V_{O2}\rightarrow V_{O4}$	0.30	1.56
$V_{O3}\rightarrow V_{O4}$	0.78	1.56

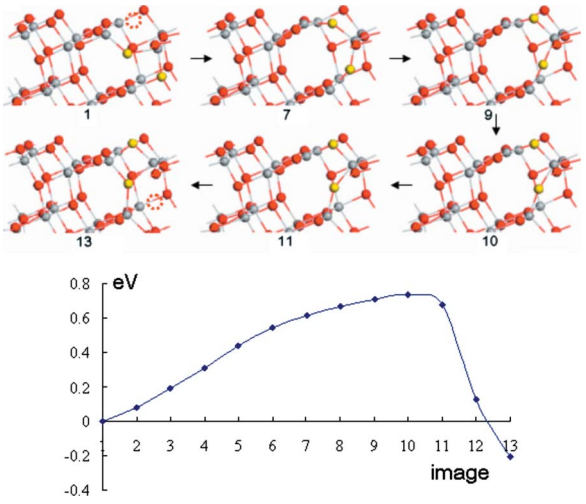

FIG. 3. (Color online) Potential energy profile along the $V_{O1} \rightarrow V_{O4}$ diffusion pathway. In the upper part of the figure selected atomic configurations (NEB "images") along the pathway are shown. The initial and final positions of the vacancy are indicated by a dashed red circle; the two oxygen which undergo the larger displacements in the diffusion process are highlighted in yellow.

A-TiO_2(101) and also on **A**-TiO_2(001), the V_O defect with the lowest formation energy is the one deepest inside the slab. However, even with some caution related to the different slab models used for the calculations, we can remark also some differences between these two **A**-TiO_2 surfaces, namely: (i) the formation energies of V_O defects on **A**-TiO_2(001) are, on average, larger than on **A**-TiO_2(101), and (ii) the "surface" region (i.e., where the defect formation energies are larger) is somewhat thicker on **A**-TiO_2(001). Both these differences appear to be consistent with the experimental UPS results.[7]

Additional comparison of the results in Table I for the two **A**-TiO_2 surfaces with those for **R**-TiO_2(110) (which agree well with recent DFT calculations[20]) clearly suggests important differences in the defect distribution at the surfaces of these two TiO_2 polymorphs. At **R**-TiO_2(110), defect formation energies in the first O-Ti-O trilayer are the lowest ones, whereas those for the second trilayer are quite high. Altogether, we can expect that most O vacancies will occur at the V_{O1} bridging and V_{O3} sub-bridging sites at **R**-TiO_2(110), in the near subsurface (V_{O4} site) and below at **A**-TiO_2(101), and only well below the surface at **A**-TiO_2(001). Again, these results appear to correlate well with the UPS findings of Ref. 7.

In summary, we have presented first-principles calculations indicating that the surface vs subsurface distribution of V_O defects in **A**-TiO_2 is quite different from that at **R**-TiO_2(110). In **A**-TiO_2, O vacancies are found to have a substantially lower probability to form at the surface than in the subsurface region, whereas surface bridging and subbridging V_O's are most likely at **R**-TiO_2(110). While it will be important to confirm these conclusions using electronic structure calculations that overcome the limitations of the present DFT-GGA approach, the present results on the qualitative differences between anatase and rutile appear to be fully consistent with the experiment and provide a clear explanation of a variety of experimental findings.

We thank U. Diebold, C. Di Valentin, G. Pacchioni, and A. Vittadini for comments and discussions. We acknowledge the Department of Energy for financial support (Contract No. DE-FG02-05ER15702) and Keck Computational Materials Science Laboratory in Princeton for computing time.

[1] A. L. Linsebigler, G. Lu, and J. T. Yates, Jr., Chem. Rev. (Washington, D.C.) **95**, 735 (1995).
[2] M. Grätzel, Nature (London) **414**, 338 (2001).
[3] U. Diebold, Surf. Sci. Rep. **48**, 53 (2003).
[4] M. R. Ranade, A. Navrotsky, H. Z. Zhang *et al.*, Proc. Natl. Acad. Sci. U.S.A. **99**, 6476 (2002).
[5] H. Z. Zhang and J. F. Banfield, J. Mater. Chem. **8**, 2073 (1998).
[6] M. Lazzeri, A. Vittadini, and A. Selloni, Phys. Rev. B **63**, 155409 (2001).
[7] A. G. Thomas, W. R. Flavell, A. K. Mallick *et al.*, Phys. Rev. B **75**, 035105 (2007).
[8] S. Wendt, R. Schaub, J. Matthiesen *et al.*, Surf. Sci. **598**, 226 (2005).
[9] O. Bikondoa, C. L. Pang, R. Ithnin, C. A. Muryn, H. Onishi, and G. Thornton, Nature Mater. **5**, 189 (2006).
[10] C. Di Valentin, G. Pacchioni, and A. Selloni, Phys. Rev. Lett. **97**, 166803 (2006).
[11] M. V. Ganduglia-Pirovano, A. Hofmann, and J. Sauer, Surf. Sci. Rep. **62**, 219 (2007).
[12] Z. Zhang, Q. Ge, S. C. Li, B. D. Kay, J. M. White, and Z. Dohnalek, Phys. Rev. Lett. **99**, 126105 (2007).
[13] P. Kruger, S. Bourgeois, B. Domenichini *et al.*, Phys. Rev. Lett. **100**, 055501 (2008).
[14] M. A. Henderson, Surf. Sci. **419**, 174 (1999).
[15] O. Warschkow, Y. Wang, A. Subramanian, M. Asta, and L. D. Marks, Phys. Rev. Lett. **100**, 086102 (2008).
[16] A. Vittadini and A. Selloni, J. Chem. Phys. **117**, 353 (2002).
[17] J. Oviedo, M. A. San Miguel, and J. F. Sanz, J. Chem. Phys. **121**, 7427 (2004).
[18] M. D. Rasmussen, L. M. Molina, and B. Hammer, J. Chem. Phys. **120**, 988 (2004).
[19] T. Pabisiak and A. Kiejna, Solid State Commun. **144**, 324 (2007).
[20] D. J. Shu, S. T. Ge, M. Wang, and N. B. Ming, Phys. Rev. Lett. **101**, 116102 (2008).
[21] Y. Han, C. J. Liu, and Q. Ge, J. Phys. Chem. C **111**, 16397 (2007).
[22] C. J. Calzado, N. C. Hernandez, and Javier Fdez. Sanz, Phys. Rev. B **77**, 045118 (2008).
[23] B. J. Morgan and G. W. Watson, Surf. Sci. **601**, 5034 (2007).
[24] E. Finazzi, C. Di Valentin, G. Pacchioni, and A. Selloni, J. Chem. Phys. **129**, 154113 (2008).
[25] A. J. Cohen, P. Mori-Sanchez, and W. Yang, Science **321**, 792 (2008).
[26] J. P. Perdew, K. Burke, and M. Ernzerhof, Phys. Rev. Lett. **77**, 3865 (1996).
[27] S. Baroni, P. Giannozzi, S. De Gironcoli *et al.*, (URL: http://www.democritos.it).
[28] D. Vanderbilt, Phys. Rev. B **41**, 7892 (1990).
[29] M. Lazzeri and A. Selloni, Phys. Rev. Lett. **87**, 266105 (2001).
[30] G. Henkelman, B. P. Uberuaga, and H. Jonsson, J. Chem. Phys. **113**, 9901 (2000).